Journal of Molecular Structure 976 (2010) 333–341

Contents lists available at ScienceDirect

Journal of Molecular Structure

journal homepage: www.elsevier.com/locate/molstruc

Infrared spectra of methyl isocyanate isolated in Ar, Xe and N_2 matrices

Igor Reva [a,*], Leszek Lapinski [a,b], Rui Fausto [a]

[a] Department of Chemistry, University of Coimbra, 3004-535 Coimbra, Portugal
[b] Institute of Physics, Polish Academy of Sciences, 02-668 Warsaw, Poland

ARTICLE INFO

Article history:
Received 31 January 2010
Received in revised form 24 March 2010
Accepted 25 March 2010
Available online 2 April 2010

Dedicated to Professor Austin J. Barnes on the occasion of his 65th birthday.

Keywords:
Methyl isocyanate
Matrix isolation
Infrared spectra
Vibrational coupling
Anharmonic calculations

ABSTRACT

The infrared spectra of methyl isocyanate monomer isolated in cryogenic argon, xenon and nitrogen matrices were studied. Interpretation of the experimental results was supported by harmonic and anharmonic calculations carried out at the DFT, MP2 and CCSD levels of approximation. Spectral indicators of the molecule structural flexibility were examined, the most striking of these being the multiplet structure of the most intense infrared band due to the antisymmetric stretching vibration of the N═C═O group. The observed quadruplet, spanning over the frequency range of nearly 100 cm^{-1}, between 2350 and 2250 cm^{-1}, was interpreted in terms of coupling with the low frequency torsion of the methyl group.

1. Introduction

Methyl Isocyanate (O═C═N─CH_3; MIC) is used in the production of synthetic rubber, polyurethane foams, plastics, adhesives, pesticides and herbicide intermediates [1–3]. It is also currently used for the conversion of aldoximes to nitriles. MIC is an extremely toxic compound by inhalation, ingestion and skin absorption [4–6]. It may affect animals [7,8], plants [9,10] and soils [11,12]. The toxic effect of the compound on humans manifested itself when around 40 tonnes of MIC were accidentally released at a Union Carbide plant in Bhopal, India, in 1984, killing thousands [13,14]. The hazardous effects of MIC have been extensively studied [15–17]. Nowadays, due to the concerns of the public safety, there are efforts at global scale to reduce its production [18].

From the fundamental point of view, the compound has also been extensively studied. The first electron diffraction spectrum of MIC was reported as early as in 1940 (!) [19], and has been re-investigated later, in 1972 [20]. The microwave spectrum of MIC has been observed by Curl et al. [21], Lett and Flygare [22] and, more recently, by Kreglewski [23,24], Kasten and Dreizler [25] and Koput [26–28]. Koput also reported a series of theoretical studies on this subject [28–30]. MIC was found to be an asymmetric top molecule with a CNC valence angle of about 140°. The barrier for methyl torsion was found to be only 22 cm^{-1}, whereas the barrier to linearity of the CNC skeleton was determined as 920 cm^{-1}. Methyl torsion and CNC bending correspond both to large amplitude motions and the respective energy levels were experimentally accessed by microwave spectroscopy [28,30].

The structure of MIC, barriers to internal rotation as well as the vibrational spectra of this compound have been the subject of several computational studies [30–34]. Experimental infrared and Raman spectra of gaseous, liquid and solid MIC were also reported [34,35].

In the present work, we investigated the infrared spectra of monomeric MIC molecules isolated in cryogenic Ar, Xe and N_2 matrices. We are not aware of any previous report on experimental studies of MIC isolated in low-temperature inert gas environment. The current investigation revealed unusual absorption signatures of MIC, reflecting strong anharmonicity and large-amplitude character of some vibrations in this molecule. The experimental mid-infrared FTIR spectra of monomeric MIC were interpreted with the aid of harmonic and anharmonic vibrational calculations.

2. Experimental procedure

The sample of methyl isocyanate was purchased from Supelco. The commercial sealed glass ampoule containing 500 mg of the liquid compound was placed into a section of a glass vacuum line. This section was evacuated and then cut from the vacuum pumps. The ampoule was broken under static vacuum. The vapor pressure of methyl isocyanate at 20 °C is high (348 mm Hg), therefore the

* Corresponding author. Tel.: +351 967 215 641; fax: +351 239 827 703.
E-mail address: reva@qui.uc.pt (I. Reva).

0022-2860/$ - see front matter © 2010 Elsevier B.V. All rights reserved.
doi:10.1016/j.molstruc.2010.03.081

liquid compound turned instantly into gas. Argon N60, xenon N45 and nitrogen N50 (all supplied by Air Liquide) were used as the matrix gas (MG) hosts. Mixtures of gaseous MIC and a large (800–1000 fold) excess of MG were prepared using standard manometric techniques. The MG:MIC mixtures were deposited onto a cooled CsI window that was used as the optical substrate for matrices. Temperature of the CsI window was measured directly at the sample holder by a silicon diode temperature sensor connected to a digital temperature controller (Scientific Instruments, Model 9650-1), which provides accuracy of 0.1 K. All experiments have been done on the basis of the APD Cryogenics closed-cycle helium refrigeration system with a DE-202A expander. Spectra were recorded, in the 4000–400 cm^{-1} range with 0.5 cm^{-1} resolution, on a Mattson FTIR spectrometer (Infinity 60AR series) equipped with a DTGS detector and KBr beamsplitter. Necessary modifications of the sample compartment of the spectrometer were made in order to accommodate the cryostat head and allow efficient purging of the instrument by a stream of dry air to exclude influence of atmospheric H_2O and CO_2.

3. Theoretical methods

In the present study, both DFT and correlated-level ab initio methods were used to optimize the molecular geometry and calculate vibrational frequencies. The DFT calculations were performed with the B3LYP three-parameter density functional, which includes Becke's gradient exchange correction [36], the Lee, Yang, Parr correlation functional [37], and the Vosko, Wilk, Nusair correlation functional [38]. The standard Dunning's correlation-consistent polarized double-ζ basis set augmented with s and p diffuse functions on hydrogen and s, p and d diffuse functions on heavy atoms (aug-cc-pVDZ) and triple-ζ basis set augmented with s, p and d diffuse functions on hydrogen and s, p, d and f diffuse functions on heavy atoms (aug-cc-pVTZ) [39–41] were used in the calculations. Geometry optimization and vibrational calculations were also carried out at the CCSD level [42,43].

The molecular geometry was fully optimized at the CCSD/aug-cc-pVDZ, B3LYP/aug-cc-pVTZ and MP2/aug-cc-pVTZ levels of theory with the "tight" convergence threshold criteria. After geometry optimization, calculation of the harmonic vibrational frequencies was carried out at the same level of theory. The precise nature of the optimized stationary points was determined by analysis of the corresponding Hessian matrices. The structures exhibiting either zero or one imaginary frequency in the calculated spectrum were characterized as minima or first-order saddle points, respectively.

The calculated frequencies were used to assist the analysis of the experimental spectra. To correct for the systematic shortcomings of the applied methodology (mainly for anharmonicity), the calculated harmonic wavenumbers were scaled down by a factor of 0.957 for the CH stretching vibrations and by a factor of 0.977 for all remaining vibrations. Additionally, the B3LYP/aug-cc-pVTZ level was also used to calculate the anharmonic vibrational frequencies. The theoretical normal modes were analyzed by means of the potential energy distribution (PED) calculations. Transformations of the force constants with respect to the Cartesian coordinates to the force constants with respect to the molecule-fixed internal coordinates allowed the PED analysis to be carried out as described by Schachtschneider and Mortimer [44]. The atom numbering and internal coordinates used in these calculations are given in Scheme 1 and Table 1, respectively. All calculations in this work were done using the Gaussian 03 program [45].

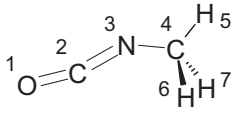

Scheme 1. Molecule of methyl isocyanate and atom numbering used in this work.

Table 1
Internal coordinates used in the normal mode analysis of methyl isocyanate (atom numbering as in Scheme 1).

A′	
$S_1 = (6^{-1/2})(2r_{4,5}-r_{4,6}-r_{4,7})$	ν_1 CH
$S_2 = (3^{-1/2})(r_{4,5}+r_{4,6}+r_{4,7})$	ν_2 CH
$S_3 = (2^{-1/2})(r_{1,2}-r_{2,3})$	ν_a N=C=O
$S_4 = (6^{-1/2})(2\beta_{7,6,4}-\beta_{5,6,4}-\beta_{5,7,4})$	β_1 CH_3
$S_5 = (2^{-1/2})(r_{1,2}+r_{2,3})$	ν_s N=C=O
$S_6 = (6^{-1/2})(\beta_{7,6,4}+\beta_{5,6,4}+\beta_{5,7,4}-\beta_{3,5,4}-\beta_{3,6,4}-\beta_{3,7,4})$	β_2 CH_3
$S_7 = (6^{-1/2})(2\beta_{3,5,4}-\beta_{3,6,4}-\beta_{3,7,4})$	β_3 CH_3
$S_8 = r_{3,4}$	ν N–C
$S_9 = \beta_{1,3,2}$ (in the symmetry plane)	β_{ip} N=C=O
$S_{10} = \beta_{2,4,3}$	β CNC
A″	
$S_{11} = (2^{-1/2})(r_{4,6}-r_{4,7})$	ν_3 CH
$S_{12} = (2^{-1/2})(\beta_{3,6,4}-\beta_{3,7,4})$	β_4 CH_3
$S_{13} = (2^{-1/2})(\beta_{5,6,4}-\beta_{5,7,4})$	β_5 CH_3
$S_{14} = \beta_{1,3,2}$ (perpendicular to the symmetry plane)	β_{oop} N=C=O
$S_{15} = (3^{-1/2})(\tau_{2,3,4,5}+\tau_{2,3,4,6}+\tau_{2,3,4,7})$	τ CH_3

$r_{i,j}$ is the distance between atoms A_i and A_j; $\beta_{i,j,k}$ is the angle between vectors A_kA_i and A_kA_j; $\tau_{i,j,k,l}$ is the dihedral angle between the plane defined by A_i, A_j, A_k and the plane defined by A_j, A_k, A_l atoms.

4. Results and discussion

The experimental FTIR spectrum of MIC isolated in an argon matrix at 8 K is shown in Fig. 1, where it is compared with the theoretically calculated spectrum. The distinctive feature of the infrared spectrum of MIC is the extremely strong band due to the antisymmetric N=C=O stretching vibration that appears around 2300 cm^{-1} and dominates the spectrum. The band exhibits a multiplet structure, which will be addressed later in this paper. The huge intensity of this band is ca. 1.5–2 orders of magnitude higher than for any other absorption.

In order to reproduce reliably this intensity difference and avoid saturation of the strongest absorption peaks, the experimental samples should be thin. The thickness of the matrix can be determined from the pattern of the interference fringes [46–48]. For the normally incident beam of the spectrometer, the basic equation for interference fringes is:

$$d = m/[2n(\nu_1 - \nu_2)],$$

where d is the film thickness; n is the refractive index of the film material; m is the number of fringes observed in the wavenumber range between ν_1 and ν_2, expressed in cm^{-1}. The refractive index for solid argon is known [49, 50]. As it follows from Fig. 1, ten full fringes were registered in the range between 3902 and 512 cm^{-1}. Then, considering that n = 1.285, the sample thickness can be estimated as 11.5 μm only. This value is about one order of magnitude less than for an average sample studied in our setup.

The fingerprint region of the FTIR spectra of MIC isolated in argon, xenon and nitrogen matrices [51] is presented in Fig. 2. The experimental spectra are very well reproduced in this range by harmonic DFT calculation, with the best match observed for the case of MIC isolated in N_2. It should be also noted that the absolute amount of MIC isolated in argon, xenon and nitrogen matrices relates roughly as 1:2:3, respectively. This ratio is reflected by the corresponding absorbance scales in Fig. 2. Taking into account that the concentrations of all samples are approximately equal, this also means that the nitrogen matrix is the thickest. Indeed, the pattern of interference fringes in nitrogen agrees with this conclusion.

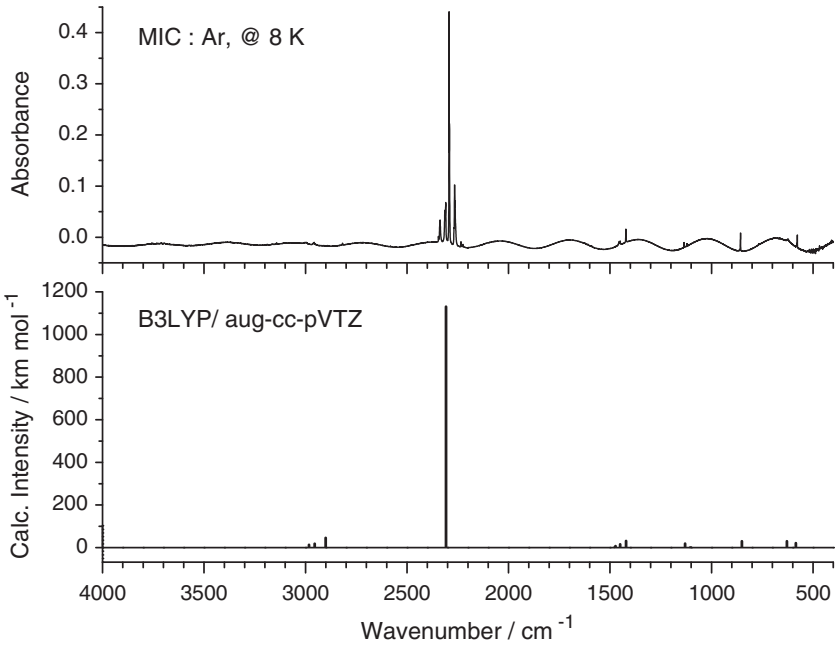

Fig. 1. Experimental FTIR spectrum of MIC monomers isolated in an argon matrix at 8 K compared with the theoretical stick spectrum calculated at the B3LYP/aug-cc-pVTZ level. Theoretical wavenumbers were scaled by a factor of 0.957 (for the CH stretching vibrations) and by a factor of 0.977 (for all the remaining vibrations).

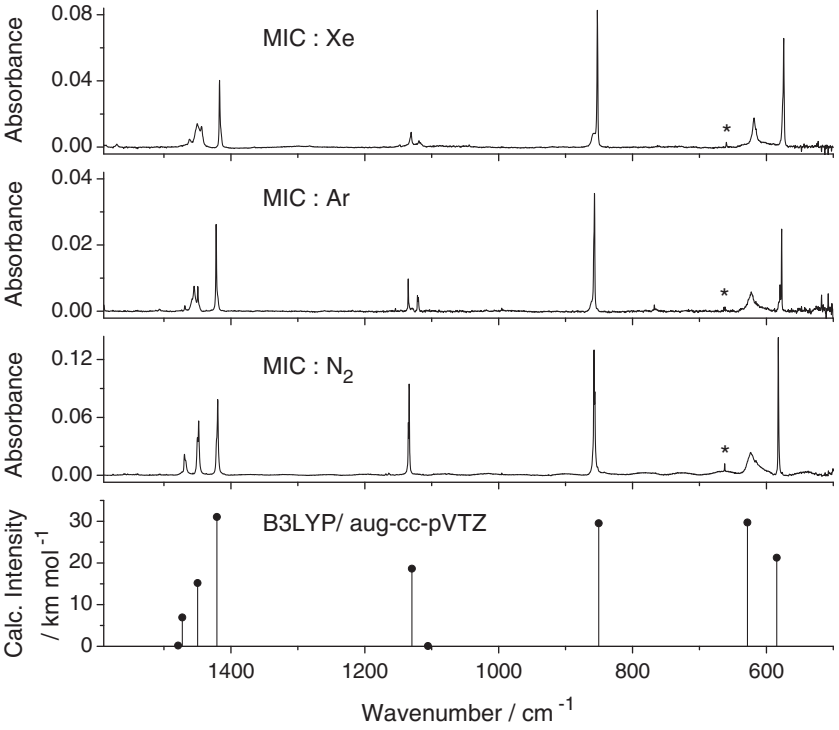

Fig. 2. The fingerprint region of the experimental FTIR spectra of MIC monomers isolated in xenon (20 K, 1:1000), argon (8 K, 1:850) and nitrogen (8 K, 1:850) matrices compared with the theoretical stick spectrum calculated at the B3LYP/aug-cc-pVTZ level. Theoretical wavenumbers in this range were scaled by a factor of 0.977 obtained from the least squares linear fit ($R = 0.99995$). Asterisks in the experimental spectra designate bands due to traces of the matrix-isolated CO_2 impurity.

In Fig. 3, the infrared spectrum of MIC isolated in a nitrogen matrix is compared with its theoretical spectra, calculated using three different models of theory. The absorption bands with maxima at 1469.3, 1448.0, 1419.8, 1133.7, 857.5 and 582.1 cm^{-1} in the spectrum of MIC isolated in a nitrogen matrix (see the assignment in Table 2) were used as references in the least squares linear fit of the theoretically calculated vibrational frequencies. As far as the overall agreement is concerned, the experimental spectrum is somewhat better reproduced by the results of the B3LYP/aug-cc-pVTZ calculation, than by the results of the calculations carried out at the MP2/aug-cc-pVTZ and CCSD/aug-cc-pVDZ levels [52]. The common scaling factor of 0.977 resulting from the best linear fit (for the B3LYP method) was then used in Fig. 3 to compare all theoretical calculations.

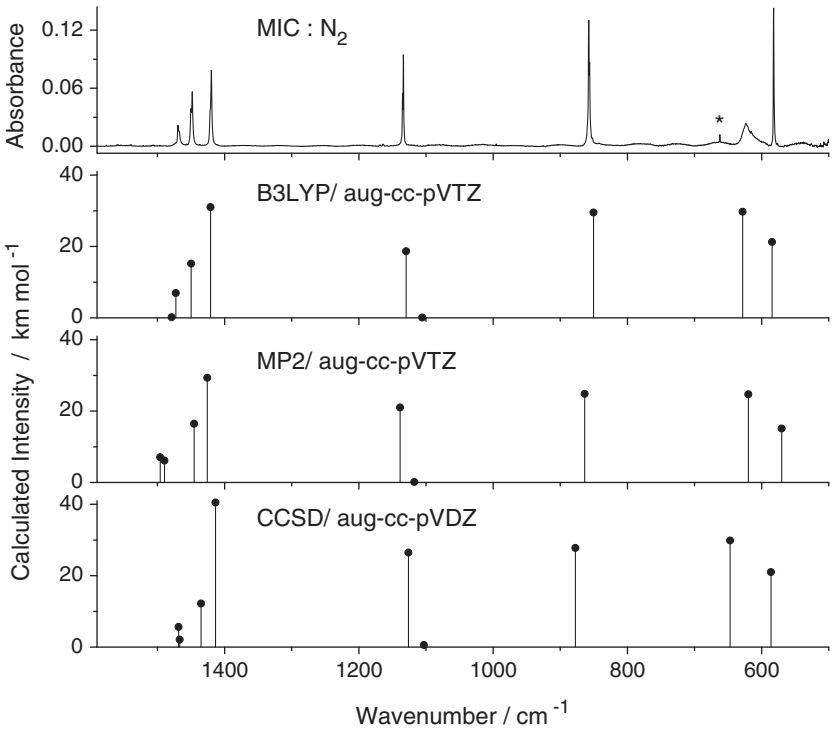

Fig. 3. Fingerprint region of the experimental FTIR spectrum of MIC monomers isolated in a nitrogen matrix at 8 K compared with the spectra calculated at the B3LYP/aug-cc-pVTZ, MP2/aug-cc-pVTZ, and CCSD/aug-cc-pVDZ levels of theory. Theoretical wavenumbers in this range were scaled by a factor of 0.977, uniform for all methods. Asterisk in the experimental spectrum designates a band due to traces of the matrix-isolated CO_2 impurity.

Table 2
Experimental wavenumbers ($\tilde{\nu}_{exp}$, cm^{-1}) and relative integrated intensities (I) of the bands in the spectrum of methyl isocyanate isolated in a nitrogen matrix, compared with theoretically calculated anharmonic ($\tilde{\nu}_{anh}$, cm^{-1}) and harmonic ($\tilde{\nu}_{har}$, cm^{-1}) wavenumbers, absolute intensities (Ath, km mol^{-1}) and potential energy distribution (PED, %).

Experimental		Calculated DFT(B3LYP)/aug-cc-pVTZ			
$\tilde{\nu}_{exp}$[a]	I[b]	$\tilde{\nu}_{anh}$[c]	$\tilde{\nu}_{har}$[d]	Ath	PED[e]
A′					
[f]	[f]	2959.6	2983.0	13	ν_1 CH(95)
[f]	82.5[f]	2931.5	2900.8	46	ν_2 CH(95)
2334.7, 2307.9, **2288.9**, 2265.2, 2259.7	1118.0[g]	2317.2	2307.7	1131	ν_a N═C═O(97)
n.o.	n.o.	1495.4	1478.7	0.2	ν_s N═C═O(40), β_2 CH_3(22), β_1 CH_3(13), β_3 CH_3(11), ν N–C(11)
1450.0, **1448.0**	19.2	1451.3	1449.6	15	β_1 CH_3(76), ν_s N═C═O(22)
1421.5 sh., **1419.8**	22.3	1425.7	1420.9	31	β_2 CH_3(86), ν_s N═C═O(11)
1134.9, **1133.7**	17.4	1134.5	1129.6	19	β_3 CH_3(88)
857.5, 856.2	32.3	850.1	850.4	30	ν N–C(75), ν_s N═C═O(27)
623.4	40.2	640.4	628.2	30	β_{ip} N═C═O(92)
n.i.	n.i.	167.3	165.2	17	β CNC(97)
A″					
[f]	[f]	2947.2	2955.0	18	ν_3 CH(100)
1469.3, 1467.6	6.0	1467.6	1472.5	7	β_5 CH_3(92)
n.o.	n.o.	1117.0	1105.7	0.1	β_4 CH_3(93)
582.1	22.1	592.6	584.4	21	β_{oop} N═C═O(107)
n.i.	n.i.	25.6	38.8	2	τ CH_3(108)

[a] The strongest component in multiplet bands is shown in bold.
[b] Relative intensity units are chosen so that their sum matches the sum of the theoretical intensities.
[c] Anharmonic wavenumbers are not scaled.
[d] Theoretical harmonic wavenumbers were scaled by a factor of 0.957 for the CH stretching vibrations and by a factor of 0.977 for all remaining vibrations.
[e] PED's lower than 10% are not included. Internal coordinates used in the normal mode analysis are given in Table 1.
[f] Due to the strong anharmonicity, assignment of the individual peaks is difficult. The integrated intensity of the CH stretching vibrations was measured over the range 3034–2742 cm^{-1}. The graphical representation of the CH stretching region is given in Fig. 9.
[g] The integrated intensity of the N═C═O antisymmetric stretching vibrations was measured over the range 2358–2235 cm^{-1}. See text for the assignments of the individual components; abbreviations: sh. – shoulder, n.o. – not observed, n.i. – not investigated.

Two vibrational modes corresponding to the bending deformations of the isocyano N═C═O group are theoretically predicted to have frequencies of ca. 600 cm^{-1}. According to the calculations, the mode at higher frequency should be due to the in-plane bending (β_{ip} N═C═O) motion, whereas that at lower frequency should correspond to the out-of-plane bending (β_{oop} N═C═O) vibration.

In agreement with the theoretical prediction, a pair of infrared absorption bands was observed in the 640–570 cm^{-1} frequency range of the experimental spectra of matrix-isolated MIC. As it is apparent form the spectra shown in Fig. 2 the shapes of these two bands are very different. The band due to the out-of-plane bending vibration [observed at 584.1 cm^{-1} (N_2)] is very narrow, whereas the band due to the in-plane bending mode [observed at 623.4 cm^{-1} (N_2)] is very broad. The broad profile of the latter band is very different from the profiles of other absorptions observed in the fingerprint region of the spectrum. The broad shape of the band at ca. 620 cm^{-1} is common to the spectra of all studied samples (Fig. 2), showing only a little dependence on the nature of the matrix gas (Ar, Xe or N_2) used. This demonstrates that the observed broad profile should be related to intrinsic properties of the MIC molecule.

The relative position of the two β N=C=O modes is a spectroscopic measure of the non-linearity of the MIC molecule. A relaxed potential energy scan along the CNC bending (β CNC) coordinate is presented in Fig. 4 (lower frame). The expected calculated frequencies of the two N=C=O bending modes, as a function of the β CNC coordinate, are shown in the upper frame. The observed broad profile of the β_{ip} N=C=O absorption band demonstrates that the molecule of MIC undergoes a large-amplitude movement in the plane of symmetry. The observed magnitude of the separation between the β_{oop} N=C=O and β_{ip} N=C=O modes indicates that the CNC angle for the matrix-isolated molecule is slightly (by 2–3°) more obtuse than predicted by the calculations. However, the molecule is clearly non-linear, because for the extreme case of the linear molecule, with C_{3v} symmetry, the frequencies of the two N=C=O bending modes would be the same (see Fig. 4). Fig. 4 shows also the two lowest β CNC vibrational levels (bending quantum numbers $v_b = 0$, $v_b = 1$) [53]. The first excited level is 2 kJ mol^{-1} higher than the ground vibrational state. Hence, for a molecule at cryogenic temperature 8–20 K (as it is the case for MIC isolated in low-temperature matrices), thermal population of the excited β CNC vibrational levels can be completely neglected. This conclusion is important for further discussion.

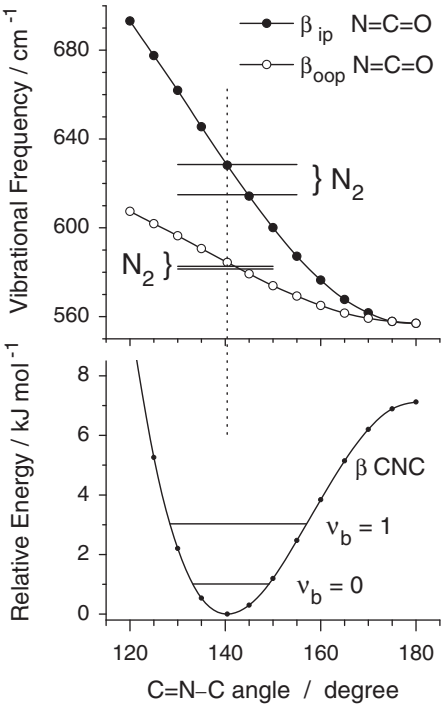

Fig. 4. Bottom: relaxed potential energy scan for bending of the MIC molecule in the symmetry plane as a function of CNC angle calculated at the B3LYP/aug-cc-pVTZ theory level. Horizontal lines designate calculated energies of the two lowest β CNC vibrational levels. The quantum numbers for the β CNC mode are designated as "bending" (v_b); top: calculated frequencies of the in-plane (β_{ip}) and out-of-plane (β_{oop}) bending vibrations of the isocyano group, scaled by a uniform factor of 0.977. The vertical dotted line designates position of the energy minimum. The pairs of horizontal lines designate the frequencies at the half-widths of the experimental absorption bands of MIC isolated in a nitrogen matrix.

The most striking feature in the infrared spectrum of matrix-isolated MIC is the band appearing around 2300 cm^{-1} (see Fig. 1). There is only one band that is expected to appear in this spectral range, due to the ν_a N=C=O mode (Table 2). The matrix isolation infrared spectra of other similar molecules bearing the N=C=O moiety show only one strong absorption. This is the case of isocyanic acid (HNCO) isolated in an argon matrix [54], HNCO isolated in matrices of krypton and xenon [55], HXeNCO isolated in a xenon matrix [56], and di-isocyanate in an argon matrix [57]. Methyl isocyanate does not stand together with the previous molecules. The experimental spectra of MIC isolated in argon, xenon and nitrogen matrices are expanded in Fig. 5. In all matrix gases, the spectrum shows a very characteristic strong absorption with a quadruplet profile spanning more than 80 cm^{-1}. The splitting of the antisymmetric N=C=O stretching vibration (between 2350 and 2250 cm^{-1}) into four components is similar in all the matrices. Therefore this splitting cannot be attributed to different packing sites in different matrix media. It is intrinsic to MIC and results from intramolecular coupling.

Before unveiling the reasons of the unusual splitting, it is interesting to establish the spectral position of the fundamental ν_a N=C=O mode. Intuitively, this should be the strongest component in the observed quadruplet. This guess is consistent with two different reasonings based on the comparison of the experiments and calculation. Let us consider them.

(i) Isotopic substitution. The bands in the spectra of matrix-isolated molecules are so narrow that it is possible to detect experimentally the absorptions due to rare isotopic forms. The IR bands originating from ^{13}C and ^{15}N rare isotopologues of matrix-isolated s-triazine [58] or ^{37}Cl minor variety of dichloropropane [59] could be identified thanks to the excellent agreement between the experimentally observed and theoretically predicted isotope shifts. In the present case, a strong infrared intensity due to ν_a N=C=O mode should allow spectral identification of the rare CH_3–N=^{13}C=O isotopologue, whose natural abundance is ca. 1%. Indeed, in the FTIR spectra of all matrices there is a group of bands around 2220–2230 cm^{-1}, having intensity ca. 1% as compared with the main peak. The corresponding absorptions are designated by brackets in Fig. 5. We calculated the isotopic shift for substitution of the central ^{12}C atom in the isocyano group by ^{13}C. For the ν_a N=C=O mode, this shift amounts to 63.5 cm^{-1} (to lower frequencies). So, the isotopic ^{13}C analysis indicates that the fundamental absorption of the main isotopic species should be expected to appear around 2285–2295 cm^{-1}, i.e. around the position where the component of the strongest intensity is observed.

(ii) Comparison with related molecules. The ν_a N=C=O mode for isocyanic acid (HNCO) isolated in an argon matrix was reliably identified as a single absorption at 2259.0 cm^{-1} [54]. Using a similar approach as described above for the isotopic analysis, we calculated the vibrational spectrum of HNCO and compared it with the calculated spectrum of MIC. In these calculations, the ν_a N=C=O mode of MIC is predicted to be 38 cm^{-1} higher than for HNCO. This gives the expectation value of 2297 cm^{-1} for MIC (in argon). The band observed in our experiments at 2293 cm^{-1} corresponds very well to the expectation and is the most intense component of the quadruplet (see Fig. 5)!

The multiplet band structure in the infrared spectra of matrix-isolated molecules can be related with the rotation of molecule in the matrix, as a whole. Isocyanic acid, for example, was found

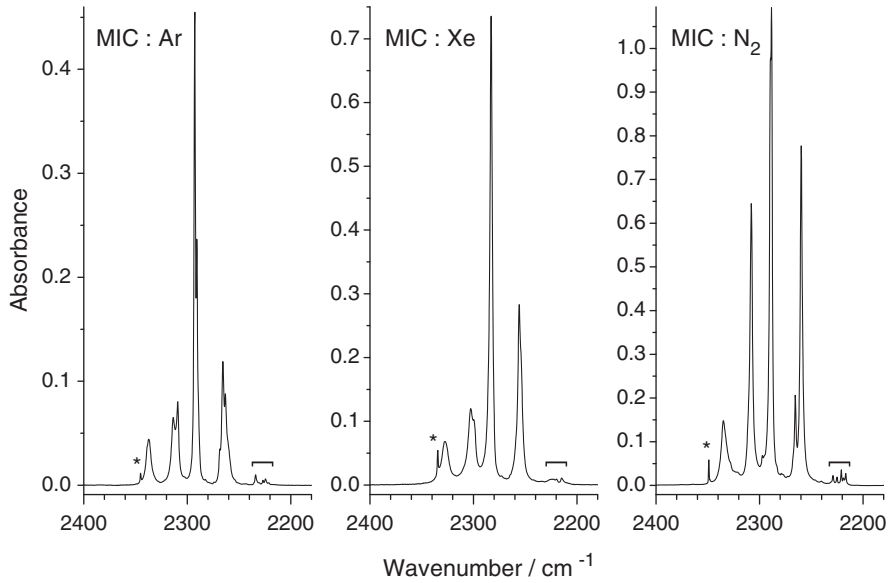

Fig. 5. Region of the antisymmetric O═C═N stretching vibration in the experimental FTIR spectra of MIC monomers isolated in argon (8 K, 1:850), xenon (20 K, 1:1000), and nitrogen (8 K, 1:850) matrices. Asterisks in the experimental spectra designate bands due to traces of the matrix-isolated CO_2 impurity. Brackets designate absorptions due to the O═^{13}C═N─CH_3 isotopologue in the natural abundance.

to rotate in an argon matrix almost freely. Several bands observed in the infrared spectrum of HNCO isolated in an argon matrix are accompanied by satellite bands, which were interpreted in terms of rotational structure of the vibrational transitions [54]. We explored this hypothesis for the case of MIC, in an attempt to explain the nature of the unusual quadruplet around 2300 cm^{-1}. For the rotating molecules, the rotational structure depends on the character of the individual bands. For pure perpendicular bands, i.e. bands where the vibrational transition dipole is perpendicular to the rotation *a* axis, the selection rule $\Delta K_a = \pm 1$ holds. For parallel bands $\Delta K_a = 0$, where K_a is the quantum number for rotation around the *a* axis. The calculated directions of the transition dipoles of MIC are presented in Fig. 6. The ν_a N═C═O dipole derivative is nearly parallel to the principal axis of inertia and should produce only a single absorption (*Q* feature). Moreover, the calculated rotational constant around the *a* axis is approximately 82.3 GHz. This value can explain a rotational structure spaced by ca. 2.7 cm^{-1}, but cannot explain the splitting which is one order of magnitude higher (see Fig. 5). Resuming, it is easy to conclude that the observed band splitting does not arise from the coupling between the ν_a N═C═O mode and the rotation of the molecule as a whole.

In a series of reports on the analysis of the microwave spectrum of MIC, Koput [27,29,30] showed that the experimental rotational spectrum can be successfully interpreted in terms of the five-dimensional quasi-symmetric top molecule model, accounting explicitly for the large-amplitude CNC bending motion, internal methyl torsion and overall rotation. On the basis of the discussion presented above, two of these three motions, the large-amplitude CNC bending and overall rotation, can be discarded as factors causing the observed splitting of the infrared band due to the ν_a N═C═O mode for matrix-isolated MIC. Let us now address the internal methyl torsion. The methyl torsion potential energy profile in MIC was calculated using MP2 and DFT methods. The results of relaxed potential-energy-scan computations carried out with several aug-cc-pVXZ (*X* = *D*, *T*, *Q*) basis sets are shown in Fig. 7. The energy barrier for methyl torsion was predicted (at all applied levels of theory) to be very low. The more complete the applied basis set is (the more basis set functions it includes), the lower is the calculated barrier for methyl torsion (see Fig. 7, left frame). In the B3LYP/aug-cc-pVTZ calculation this barrier was found to be as low

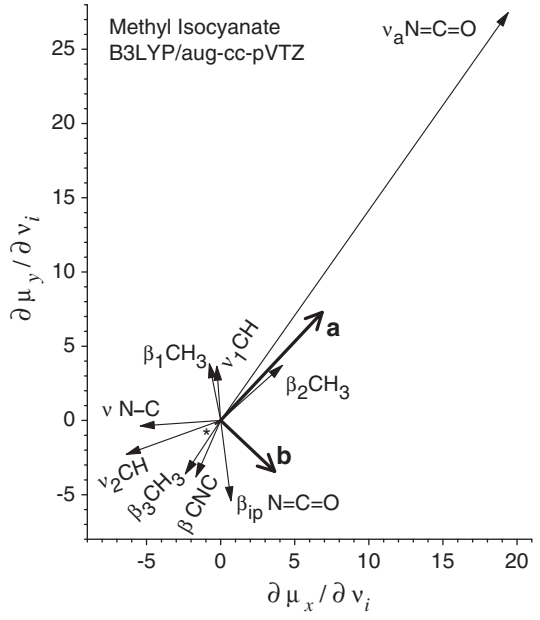

Fig. 6. Dipole derivatives for the molecule of MIC, with respect to the normal vibrations of A′ symmetry, calculated at the B3LYP/aug-cc-pVTZ theory level. The vibrational modes are designated by their major PED contribution (see Table 2). The asterisk close to the origin designates an approximate direction of the vanishing ν_s N═C═O vector. The orientations of the two principal axes of inertia, *a* and *b*, are designated by bold vectors with open arrowheads. The five *A″* modes are perpendicular to the *xy* plane and are aligned along the *z* axis, which coincides with the principal axis of inertia *c*. The coordinate system of the plot corresponds to the standard orientation of the molecule, as defined in Gaussian. The units are normalized in such a way that the lengths of the corresponding vectors, after being squared, are equal to the infrared intensity of the vibrational mode.

as 0.29 kJ mol^{-1} (24 cm^{-1}). This value is in a good agreement with the experimental estimate (22 cm^{-1}) reported by Koput [30]. In the right frame of Fig. 7, the calculated harmonic and anharmonic levels of methyl torsion are shown. Only the ground state methyl torsion level stays below the barrier. A very strong anharmonicity of the methyl torsion strikes the eye (note the mismatch between

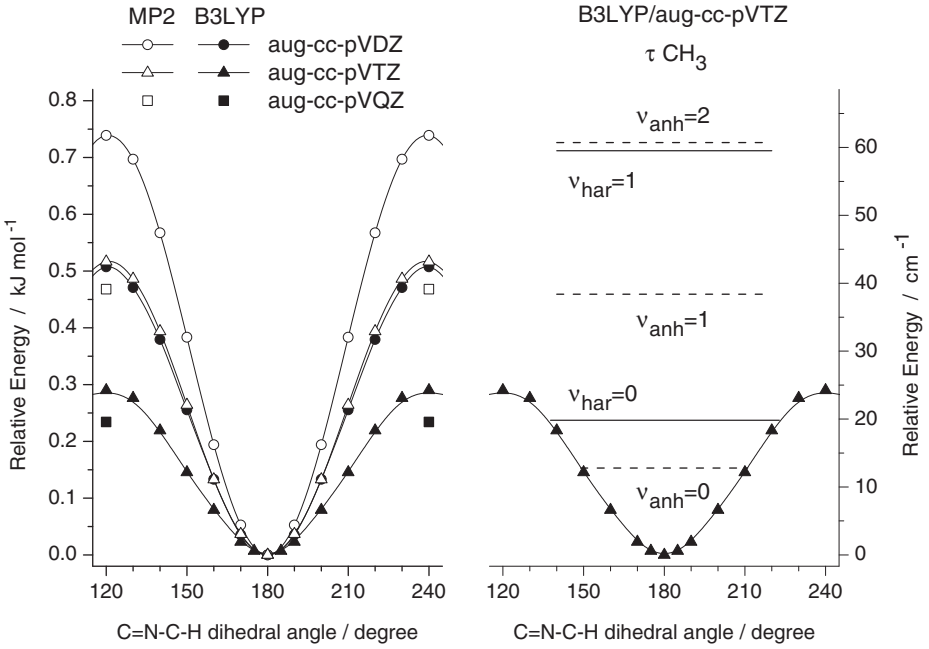

Fig. 7. Left: theoretical relaxed potential energy scans for the internal rotation of the methyl group calculated at different theory levels. The zero level of the relative energy was chosen for the staggered geometry (at the minimum). With the aug-cc-pVQZ basis, both for MP2 and DFT levels, only the stationary points were optimized. Right: B3LYP/aug-cc-pVTZ calculated relaxed potential energy scan of the methyl torsion. The horizontal bars designate the relative energies of the methyl torsion coordinate, calculated both in harmonic (solid lines) and in anharmonic (dashed lines) approximation.

the anharmonic and harmonic calculated data). The first excited methyl torsion level calculated in the anharmonic approximation was found to be as low as only 25.6 cm^{-1} over the ground state. The corresponding value extracted by Koput from the analysis of the microwave spectrum is even lower, ca. 8.3 cm^{-1} [27]. Such low-lying excited levels must be thermally populated under cryogenic conditions (estimated 6% for 25.6 cm^{-1}, at 10 K).

An easy excitation and non-negligible population of the methyl torsion levels in the low-temperature matrices prompted a simple qualitative model shown in Fig. 8. The model is expressed in a two-dimensional space of the antisymmetric N═C═O vibration (vibrational quantum numbers $v_v = 0$, $v_v = 1$) and internal methyl torsion (torsional quantum numbers $v_t = 0$, $v_t = 1$, $v_t = 2$). The transitions always occur from the ground state $v_v = 0$ to the first excited state $v_v = 1$. Combinations of different torsional quantum numbers $v_t = (0, 1)$ in the ground v_v state and $v_t = (0, 1, 2)$ in the excited v_v state allow explanation of the quadruplet structure of the manifold. An approximate spacing of 25 cm^{-1} between energy levels with consecutive v_t quantum numbers (as it is applied in the model) is in a good qualitative agreement with the spacing between the components of the quadruplet observed in the experiment. Moreover, the anharmonic prediction of $\Delta v_t = 25.6$ cm^{-1} looks also consistent with the present experiment. It should also be noted here that the proposed model explains well not only the number of components – four – in the observed multiplet, but also their relative intensities. This model confirms the finding obtained on the basis of isotopic analysis – that the most intense component of the quadruplet corresponds to the fundamental vibrational ν_a N═C═O transition. Finally, there is no experimental indication of vibrational coupling between ν_a N═C═O and β CNC modes. Indeed, the lowest excitation of the $\Delta\nu_b$ should be more than 165 cm^{-1} (see Table 2) and no band is observed in the present experiments around 2450 cm^{-1}, which is an expected position for a transition from ($v_v = 0$, $v_b = 0$) to ($v_v = 1$, $v_b = 1$).

The 3400–2650 cm^{-1} spectral range is shown in Fig. 9. It must be noted that the experimental absorbance scales in Fig. 9 refer to the same spectra as shown in Figs. 2 and 5. The average absorption intensities in this range are rather low. For the case of nitrogen matrix, which has a higher amount of the compound in the matrix and a better signal-to-noise ratio, more than 15 individual maxima

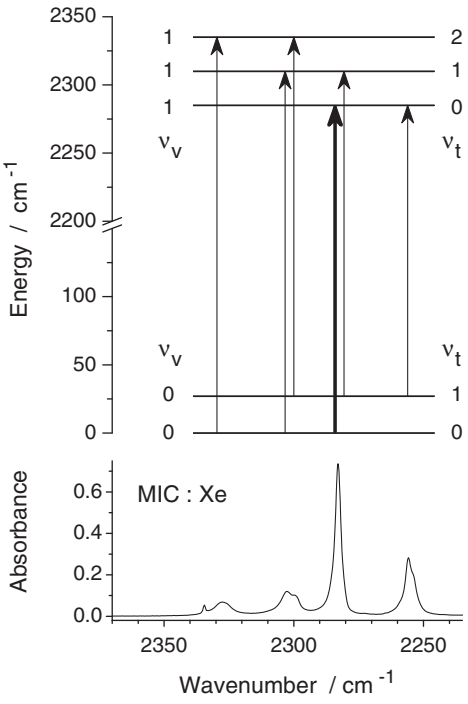

Fig. 8. Energy level scheme explaining the observed quadruplet profile in the infrared spectra of matrix-isolated methyl isocyanate. The vertical arrows showing the proposed transitions are positioned over the corresponding absorption bands in the spectrum of MIC isolated in a xenon matrix. The most probable transition is shown by the bold arrow. The quantum numbers for the ν_a N═C═O mode are designated as "vibrational" (v_v), and for the τ CH_3 mode – as "torsional" (v_t). Positions of v_v and v_t along the energy scale should be considered as qualitative.

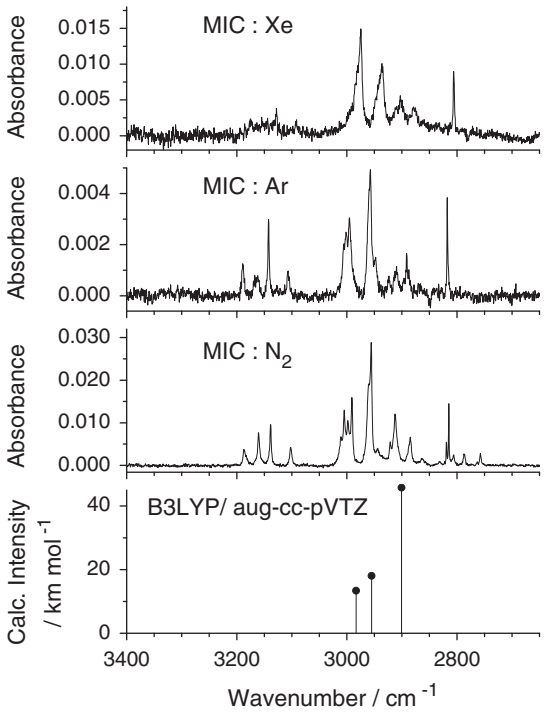

Fig. 9. Region of the CH stretching vibrations in the experimental FTIR spectra of MIC monomers isolated in xenon (20 K, 1:1000), argon (8 K, 1:850) and nitrogen (8 K, 1:850) matrices compared with the theoretical stick spectrum calculated at the B3LYP/aug-cc-pVTZ level. Theoretical wavenumbers in this range were scaled by a factor of 0.957.

can be identified in this range, while only three fundamental modes, due to the CH stretching vibrations, fall herein. The complexity of the spectrum in the CH str region does not allow for an easy assignment in this range.

It is well-known that the vibrational spectra of methyl-containing compounds can be complicated by occurrence of two types of anharmonic interactions: (i) resonances between ν CH and the first overtone (2 β CH) and/or combination tones of methyl bending (β CH) modes [60,61] and (ii) coupling of ν CH with τCH_3 modes [62,63], giving rise to polyads of levels in the 3000–2800 cm^{-1} range [64]. The assignment of the particular modes in such spectra usually requires studies of the partially deuterated CHD_2 or CH_2D analogues [65,66] and sophisticated theoretical treatment [67,68]. It is not new that MIC is amongst the molecules exhibiting a strong resonance between the ν CH and 2β CH modes [69]. Moreover, Zhou and Durig have recently reported [35] the positions of all three of the CH_3 stretching modes of MIC to have significant differences in frequencies with the changes of phase (for gaseous, liquid and solid MIC), which does not help in the interpretation of the present matrix-isolation experimental data.

The conventional harmonic vibrational calculations do not add clarity to the interpretation of this spectral region either. In order to obtain a good prediction of the frequencies a different scale factor from that used to scale down the calculated frequencies in the fingerprint region must be used. Since a simple linear fit is difficult to implement in this case, the scale factor was obtained as the average ratio [anharmonic]/[harmonic] of the individual calculated CH str frequencies (see Table 2). This approach proved successful in our recent study on hydroxyacetone, where the anharmonic calculated wavenumbers differed only within a few wavenumbers from the matrix experiment [70]. In present case, the positions of anharmonic calculated frequencies were chosen as initial guess for the frequencies of the fundamental absorptions. The resulting scaling factor of 0.957 for harmonic frequencies is in a good agreement with other studies giving the scaling factors between 0.950 and 0.960 [71–73].

The scaled harmonic frequencies as well as those resulting from the anharmonic frequency calculations (see Table 2) clearly show that no CH stretching vibrations should have frequencies higher than 3000 cm^{-1}. However, in the experimental spectra of MIC a quadruplet of bands is observed in the 3100–3200 cm^{-1} range, which cannot be due to the CH stretching fundamentals. Noteworthy, this quadruplet of bands has a similar structure to that observed in the 2250–2340 cm^{-1} region (compare Figs. 5 and 9). If we assume that these two quadruplets are related and calculate how much these two quadruplets are apart from each other, the value of about 850 cm^{-1} is obtained. There is only one vibration of MIC around 850 cm^{-1} (and there are no other bands in the 650–1050 cm^{-1} range!). The mode corresponding to the experimental band at 857.7 cm^{-1} is characterized by contributions due to the ν N—C stretching and the ν_s N=C=O coordinates, or briefly [ν N—C; ν_s N=C=O] (see Table 2). Similarly to the quadruplet resulting from the [ν_a N=C=O + τCH_3] coupling, the quadruplet observed between 3200 and 3100 cm^{-1} spans a little less than 100 cm^{-1}. Hence, it looks very likely that the latter feature should be described as the combination tone [ν_a N=C=O + τCH_3] + [ν N—C; ν_s N=C=O].

5. Conclusions

Monomers of methyl isocyanate (MIC) were studied using the matrix-isolation technique combined with FTIR spectroscopy. The observed infrared spectra of MIC isolated in Ar, Xe or N_2 low-temperature matrices were interpreted by comparison with the results of harmonic and anharmonic calculations carried out at the DFT, MP2 and CCSD levels of approximation. In spite of the fact that MIC is a flexible molecule and some of its vibrations have a large-amplitude character, the IR spectrum in the 1600–400 cm^{-1} range was very well reproduced by the results of calculations carried out within the harmonic approximation. This results in a very reliable vibrational assignment. However, some clear indications of the structural flexibility of the molecule were observed in the experimental IR spectra. The most striking of these spectral features is the multiplet structure of the most intense band due to the antisymmetric stretching vibration of the N=C=O group. This band appears (in the spectra of MIC isolated in Ar, Xe or N_2 matrices) as a quadruplet spanning at ca. 2300 cm^{-1} over the frequency range of nearly 100 cm^{-1}. The very unusual structure of this band was interpreted in terms of coupling with the torsion of the methyl group, which is the lowest frequency vibration in the molecule.

References

[1] W.E. Johns, Journal of Adhesion 15 (1982) 59–67.
[2] A.K. Mohanty, M. Misra, L.T. Drzal, Composite Interfaces 8 (2001) 313–343.
[3] T.E. Arbuckle, L.E. Sever, Critical Reviews in Toxicology 28 (1998) 229–270.
[4] J. Mraz, P. Simek, D. Chvalova, H. Nohova, P. Smigolova, Chemico-Biological Interactions 148 (2004) 1–10.
[5] U. Nangia, A.M. Jana, K.M. Rao, Current Science 55 (1986) 1139–1141.
[6] J.T. James, L.C. Buettner, S.S. Hsu, Journal of Applied Toxicology 7 (1987) 147–148.
[7] W.F. Tenberge, Journal of Hazardous Materials 12 (1985) 309–311.
[8] W.J. Caspary, B. Myhr, Mutation Research 174 (1986) 285–293.
[9] G. Kumar, A.N. Sahi, S.K. Roy, Experientia 46 (1990) 1072–1075.
[10] G. Kumar, S.K. Roy, Indian Journal of Experimental Biology 28 (1990) 460–465.
[11] B. Parthipan, A. Mahadevan, Biology and Fertility of Soils 15 (1993) 79–80.
[12] B. Parthipan, A. Mahadevan, Environmental Pollution 87 (1995) 283–287.
[13] N.H. Wadia, Recent Advances in Tropical Neurology 10 (1995) 289–298.
[14] J. Jeffery, J. Sztain, S. Sarangi, T. Kuo, Journal of Investigative Medicine 54 (2006) 535.
[15] C.L. Kuckel, B.W. Lubit, P.K. Lambooy, P.N. Farnsworth, Biochimica et Biophysica Acta 1162 (1993) 143–148.
[16] G.P. Meshram, K.M. Rao, Indian Journal of Experimental Biology 25 (1987) 548–550.
[17] C.K. Lee, Journal of Biological Chemistry 251 (1976) 6226–6231.

[18] See for Example: S.D. Hamill, The New York Times (NY edition), August 27, 2009, p. A23. <http://www.nytimes.com/2009/08/27/us/27chemical.html>.
[19] E.H. Eyster, R.H. Gillette, L.O. Brockway, Journal of the American Chemical Society 62 (1940) 3236–3243.
[20] D.W.W. Anderson, D.W.H. Rankin, A. Robertson, Journal of Molecular Structure 14 (1972) 385–396.
[21] R.F. Curl Jr., V.M. Rao, K.V.L.N. Sastry, J.A. Hodgeson, Journal of Chemical Physics 39 (1963) 3335–3340.
[22] R.G. Lett, W.H. Flygare, Journal of Chemical Physics 47 (1967) 4730–4750.
[23] M. Kreglewski, Chemical Physics Letters 112 (1984) 275–278.
[24] M. Kreglewski, Journal of Molecular Spectroscopy 105 (1984) 8–23.
[25] W. Kasten, H. Dreizler, Zeitschrift Für Naturforschung Section A: Journal of Physical Sciences 41 (1986) 637–640.
[26] J. Koput, Journal of Molecular Spectroscopy 118 (1986) 448–458.
[27] J. Koput, Journal of Molecular Spectroscopy 115 (1986) 131–146.
[28] J. Koput, Journal of Molecular Spectroscopy 127 (1988) 51–60.
[29] J. Koput, Journal of Molecular Spectroscopy 106 (1984) 12–21.
[30] J. Koput, Chemical Physics Letters 242 (1995) 514–520.
[31] H.-G. Mack, H. Oberhammer, Chemical Physics Letters 157 (1989) 436–439.
[32] M.H. Palmer, P.J. Camp, Molecular Physics 101 (2003) 3053–3062.
[33] M.H. Palmer, A.D. Nelson, Journal of Molecular Structure 689 (2004) 161–173.
[34] J.F. Sullivan, H.L. Heusel, W.M. Zunic, J.R. Durig, S. Cradock, Spectrochimica Acta Part A – Molecular and Biomolecular Spectroscopy 50 (1994) 435–447.
[35] S.X. Zhou, J.R. Durig, Journal of Molecular Structure 924–926 (2009) 111–119.
[36] A.D. Becke, Physical Review A 38 (1988) 3098–3100.
[37] C.T. Lee, W.T. Yang, R.G. Parr, Physical Review B 37 (1988) 785–789.
[38] S.H. Vosko, L. Wilk, M. Nusair, Canadian Journal of Physics 58 (1980) 1200–1211.
[39] D.E. Woon, T.H. Dunning, Journal of Chemical Physics 98 (1993) 1358–1371.
[40] R.A. Kendall, T.H. Dunning, R.J. Harrison, Journal of Chemical Physics 96 (1992) 6796–6806.
[41] T.H. Dunning, Journal of Chemical Physics 90 (1989) 1007–1023.
[42] G.E. Scuseria, C.L. Janssen, H.F. Schaefer III, Journal of Chemical Physics 89 (1988) 7382–7387.
[43] J. Cížek, On the use of the cluster expansion and the technique of diagrams in calculations of correlation effects in atoms and molecules. in: P.C. Hariharan, (Ed.), Correlation Effects in Atoms and Molecules, Wiley Interscience, New York, 1969, pp 35–91.
[44] J.H. Schachtschneider, F.S. Mortimer. Vibrational Analysis of Polyatomic Molecules. VI. FORTRAN IV Programs for Solving the Vibrational Secular Equation and for the Least-Squares Refinement of Force Constants. Project No. 31450. Structural Interpretation of Spectra, Shell Development Co., Emeryville, CA, 1969.
[45] M.J. Frisch, G.W. Trucks, H.B. Schlegel, G.E. Scuseria, M.A. Robb, J.R. Cheeseman, J. Montgomery, J.A.T. Vreven, K.N. Kudin, J.C. Burant, J.M. Millam, S.S. Iyengar, J. Tomasi, V. Barone, B. Mennucci, M. Cossi, G. Scalmani, N. Rega, G.A. Petersson, H. Nakatsuji, M. Hada, M. Ehara, K. Toyota, R. Fukuda, J. Hasegawa, M. Ishida, T. Nakajima, Y. Honda, O. Kitao, H. Nakai, M. Klene, X. Li, J.E. Knox, H.P. Hratchian, J.B. Cross, V. Bakken, C. Adamo, J. Jaramillo, R. Gomperts, R.E. Stratmann, O. Yazyev, A.J. Austin, R. Cammi, C. Pomelli, J.W. Ochterski, P.Y. Ayala, K. Morokuma, G.A. Voth, P. Salvador, J.J. Dannenberg, V.G. Zakrzewski, S. Dapprich, A.D. Daniels, M.C. Strain, O. Farkas, D.K. Malick, A.D. Rabuck, K. Raghavachari, J.B. Foresman, J.V. Ortiz, Q. Cui, A.G. Baboul, S. Clifford, J. Cioslowski, B.B. Stefanov, G. Liu, A. Liashenko, P. Piskorz, I. Komaromi, R.L. Martin, D.J. Fox, T. Keith, M.A. Al-Laham, C.Y. Peng, A. Nanayakkara, M. Challacombe, P.M.W. Gill, B. Johnson, W. Chen, M.W. Wong, C. Gonzalez, J.A. Pople, Gaussian 03, Revision C.02, Gaussian, Inc., Wallingford, CT, 2004.
[46] F.E. Ghodsi, Surface Review and Letters 12 (2005) 425–431.
[47] R. Swanepoel, Journal of Physics E – Scientific Instruments 16 (1983) 1214–1222.
[48] J.M. Adee, C. Steinbrüchel, Thin Solid Films 306 (1997) 171–173.
[49] A.C. Sinnock, B.L. Smith, Physical Review 181 (1969) 1297–1307.
[50] The refractive index of solid argon at 20 K and at 643.9 nm is equal to 1.2895, as defined by Sinnock and Smith in Ref. [49]. It increases slightly with cooling, but decreases with the increase of wavelength. We extrapolated this value to 1.285 for 8 K and for the Mid-Infrared spectral range.
[51] Note that baselines of the experimental spectra were corrected in Fig. 2.
[52] The linear fittings for different theoretical methods, with intercept equal to zero, produced the following *B*, *R* and SD values. B3LYP: $B = 0.977$, $R = 0.99995$, SD = 4.11; MP2: B = 0.972, $R = 0.99963$, SD = 11.75; CCSD: $B = 0.979$, $R = 0.99969$, SD = 11.39. *B*, *R* and SD stand for the slope (i.e. scaling factor), correlation coefficient and standard deviation, respectively.
[53] In the scale of the figure, the energies calculated for the CNC bending vibration in harmonic and in anharmonic approximation are practically the same.
[54] J.H. Teles, G. Maier, B.A. Hess Jr., L.J. Schaad, M. Winnewisser, B.P. Winnewisser, Chemische Berichte 122 (1989) 753–766.
[55] M. Pettersson, L. Khriachtchev, S. Jolkkonen, M. Räsänen, Journal of Physical Chemistry A 103 (1999) 9154–9162.
[56] M. Pettersson, L. Khriachtchev, J. Lundell, S. Jolkkonen, M. Räsänen, Journal of Physical Chemistry A 104 (2000) 3579–3583.
[57] G. Maier, M. Naumann, H.P. Reisenauer, J. Eckwert, Angewandte Chemie-International Edition in English 35 (1996) 1696–1697.
[58] H. Rostkowska, L. Lapinski, M.J. Nowak, Vibrational Spectroscopy 49 (2009) 43–51.
[59] A. Olbert-Majkut, I.D. Reva, R. Fausto, Chemical Physics Letters 456 (2008) 127–134.
[60] D.C. McKean, Chemical Society Reviews 7 (1978) 399–422.
[61] J. Fernandez Bertran, B. La Serna, Spectrochimica Acta Part A – Molecular and Biomolecular Spectroscopy 45 (1989) 117–118.
[62] D. Cavagnat, L. Lespade, Journal of Chemical Physics 114 (2001) 6030–6040.
[63] D. Cavagnat, L. Lespade, Journal of Chemical Physics 114 (2001) 6041–6050.
[64] J.P. Perchard, F. Romain, Y. Bouteiller, Chemical Physics 343 (2008) 35–46.
[65] D.C. McKean, Spectrochimica Acta Part A – Molecular Spectroscopy A 29 (1973) 1559–1574.
[66] D.C. McKean, I.A. Ellis, Journal of Molecular Structure 29 (1975) 81–96.
[67] Y. Bouteiller, J.P. Perchard, Chemical Physics 360 (2009) 59–66.
[68] D. Cavagnat, L. Lespade, Journal of Physical Chemistry A 109 (2005) 4062–4072.
[69] J.C. Lavalley, N. Sheppard, Spectrochimica Acta Part A – Molecular Spectroscopy 28 (1972) 2091–2101.
[70] A. Sharma, I. Reva, R. Fausto, Journal of the American Chemical Society 131 (2009) 8752–8753.
[71] I.D. Reva, S. Jarmelo, L. Lapinski, R. Fausto, Journal of Physical Chemistry A 108 (2004) 6982–6989.
[72] I.D. Reva, S.G. Stepanian, L. Adamowicz, R. Fausto, Journal of Physical Chemistry A 107 (2003) 6351–6359.
[73] I.D. Reva, S.G. Stepanian, L. Adamowicz, R. Fausto, Journal of Physical Chemistry A 105 (2001) 4773–4780.